I-EDU GROUP

Article

Fabrication of zinc oxide nanostructures via a low-temperature method and investigation of their photoluminescence properties

Rivojiddin R.Jalolov *[1,2], **Rustamova N.Bakhora** [1]

[1] Uzbekistan Academy of Sciences, Institute of Ion-Plasma and Laser Technologies, Tashkent 100125, Uzbekistan
[2] Department of Physics, National University of Uzbekistan, Tashkent, 100174, Uzbekistan
rr_jalolov@iplt.uz (R.J.)
* Correspondence: rr_jalolov@iplt.uz; Tel.: +998 97 4272771 (R.J.)

Abstract: ZnO nanorods were successfully synthesized by the low-temperature hydrothermal method on a grid formed by cross-weaving stainless-steel wires. Our method includes seeding process by simple dip-coating technique, followed by post annealing process and hydrothermal growth process of ZnO nanostructures. When the nanorods were synthesized a second time, their size increased and the maximum of the photoluminescence spectrum shifted toward the larger wavelength. It was observed that the shift of the PL emission band was associated with the increase in the size of the nanostructures. At the same time, the photoluminescence spectra of the samples showed an increase in the emission band associated with defects. Considering that the defect observed in the PL spectrum is interstitial oxygen, the increase in the emission band corresponding to this defect in the doubly synthesized samples indicates that they are a bulk defect.

Keyword: zinc oxide, hydrothermal, photoluminescence, defect.

Introduction

The progress of modern technologies dictates ever-increasing demands for research related to the search for new materials that could meet the growing needs of electronics, photonics and other high-tech areas in the future. In this regard, there is extraordinary activity in the scientific community in the field of obtaining, studying the properties and searching for practical applications of quasi-one-dimensional (1D) nanocrystalline materials (threads, wires, rods, tubes, etc.), including those based on zinc oxide (ZnO). ZnO is a widely studied metal oxide semiconductor, due to its potential use in a variety of applications, such as gas sensors [1], transparent electrodes in solar cells [2], photocatalysts [3], nanolasers [4], photoluminescent devices [5], and organic light emitting diodes [6] and et al. A wide bandgap (3.37 eV at room temperature) makes ZnO a promising material for photonic applications in the UV and blue spectral range, while the high exciton-binding energy (60 meV) allows efficient excitonic emission even at room temperature [7]. Also, ZnO is biocompatible which makes it suitable for biomedical applications [8]. In addition, ZnO is a chemically stable and environmentally friendly material. Consequently, there is considerable interest in studying ZnO in the form of powders, single crystals, thin films and nanostructures. There are various methods for obtaining one-dimensional zinc oxide structures, the most common being chemical vapor deposition [9] and hydrothermal synthesis [10]. The vapor phase synthesis method allows one-dimensional zinc oxide structures to be obtained on various oriented substrates: silicon coated with thin metal films (Au, In) or without any coating, silicon oxide, gallium nitride, aluminum oxide. The main feature and complexity of this technique is the sufficiently high synthesis temperature required for melting and boiling of metallic zinc (419°C and 906°C, respectively).

Hydrothermal synthesis is a method for obtaining various inorganic compounds through chemical reactions in closed systems occurring in aqueous solutions at temperatures above 100 °C and pressures above 1 atm [11]. It should be noted that the main advantages of this method are high productivity, low price and ease of implementation.

Quoting: Rivojiddin R.Jalolov, Rustamova N.Bakhora. Fabrication of zinc oxide nanostructures via a low-temperature method and investigation of their photoluminescence properties. **2024**, 1,2, 3. https://doi.org/

Received: 10.12.2024
Corrected: 18.12.2024
Accepted: 25.12.2024
Published: 30.12.2024

Typically, a photoluminescence (PL) spectrum of ZnO nanostructures consists of two parts: a near band edge (NBE) emission centered at around 380 nm and defect related emission bands in the visible range [12]. The PL characteristics of ZnO nanostructures strongly depend on their crystalline quality, which in turn is determined by growing conditions and methods and post-grown treatment history. The defect related emission bands can appear in violet–blue (390–460 nm) or/and green (500–520 nm) or/and yellow–orange (560–600 nm) or/and red (650 nm) ranges. The NBE emission, in addition to the emission of free exciton recombination, can also contain bands caused by transitions to or from the defect related levels which are located near conducting or valence bands. Despite the large body of research devoted to native defects in ZnO, many questions remain regarding the optical and electronic properties of these centers.

In this work, ZnO nanorods were grown on a stainless-steel grid by a low-temperature hydrothermal method. The synthesized nanorods exhibited strong exciton luminescence, indicating a good crystalline structure. If the nanorods were synthesized in the autoclave for a second time to synthesize ZnO nanorods, their size increased. At the same time, the photoluminescence spectra of the samples showed an increase in the emission band associated with defects.

Materials and Methods

ZnO nanorods were synthesized by the low-temperature hydrothermal method on a grid formed by cross-weaving stainless-steel wires. Firstly, the substrates were cleaned in an ultrasonic bath for 15 minutes in acetone and ethanol. Then, ZnO seed layer were formed on substrates by dip coating method. Next, put the seed layer coated substrates into the oven at 3000C for 20 minutes to crystallize the seed particles. The growth procedure was designed as follows: the aqueous solutions of zinc nitrate hexahydrate and hexamethyl tetramine were first prepared separately and then they were mixed together. Then, the solution was transferred to a steel autoclave, where substrates (steel grids) with ZnO seed layer were previously placed. In the autoclave, some substrates (sample No. 1) were placed in a horizontal position and others in a vertical position (sample No. 2). Finally, the autoclave was tightly closed and placed in a thermostat bath with water. The hydrothermal reaction was carried out at 90°C for 5 hours.

Photoluminescence (PL) spectra were obtained employing a 0.75-m high-aperture monochromator and a BCI-280 boxcar integrator designed to detect pulsed signals by the gating method [10]. The samples were excited by pulsed N2 laser (337 nm, 6 ns, P 15 kW, repetition rate of 100 Hz). The morphology of the samples was studied using a scanning electron microscope (SEM) EVO M10 (Zeiss). For the structural characterizations of ZnO nanostructures, X-ray diffraction (XRD) patterns were collected on a MINIFLEX-600 diffractometer (Rigaku).

Results

The XRD pattern of ZnO nanostructures is presented in Figure 2. All the Bragg diffraction peaks (2=34.5o, 31.8o, 36.2o, 47.5o, 56.6o,) observed in the XRD spectrum belong to the hexagonal wurtzite structure of ZnO, and the value of the crystal lattice constants is fully consistent with the standard card JCPDS 36-1451 [13]. The dominance of the Bragg diffraction peak at 2= 34.4o (002) degrees in the XRD spectrum indicates that crystallization along the c-axis is an alternative in the growth of ZnO nanostructures. In the diffractogram, Bragg diffraction peaks related to other phases of ZnO or to the doped atoms were not observed.

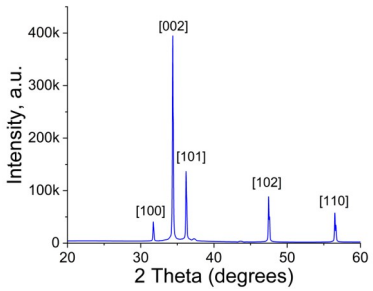

Figure 1. XRD patterns of ZnO nanostructures.

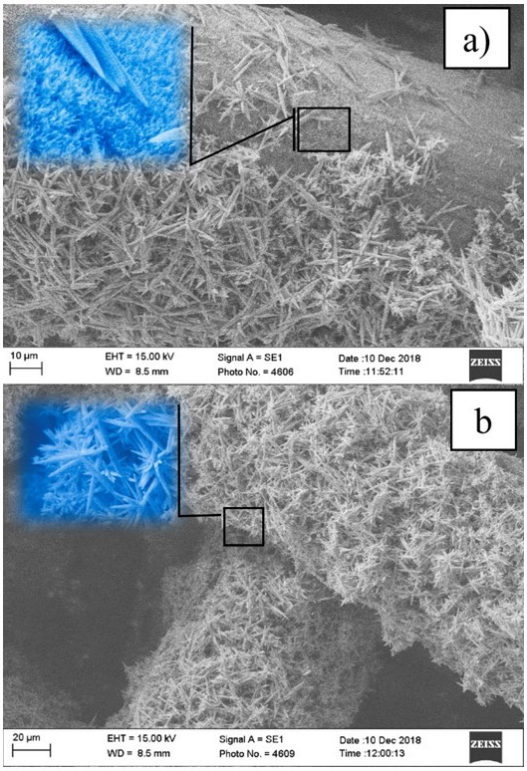

Figure 2. Micrographs of ZnO nanorods obtained by a scanning electron microscope. a - sample No. 1, b - sample No. 2

Fig. 2 shows microphotographs of a stainless-steel mesh with ZnO nanorods after repeated synthesis, obtained by a scanning electron microscope at various magnifications. As can be seen, in sample No. 1, the wire mesh is completely covered with vertically grown nanorods and horizontally located nanorods are “piled up” from above (Fig. 2a). In this process, at the same time, two nanostructure layers form on the surface of the stainless-steel mesh: the lower layer is predominantly vertically oriented relative to the surface of the nanorods grown on ZnO seed layer (insert Fig. 2a) and chaotically on top, mainly horizontally located nanorods. The horizontally located nanorods have the form of spindle-shaped rods with a decrease in diameters to both ends. The nanorods in the cross section have the correct hexagonal shape. The length of nanorods is 12-15 microns, and the diameter is 0.5-1 microns.

The synthesis of nanostructures over the entire volume of the solution simultaneously with the growth of nanorods on the seed layer leads to a uniform distribution of these nanostructures on the surface of the mesh of sample No. 2, placed vertically in the reactor (Fig. 2b). Unlike sample No. 1, the second layer of nanorods with relatively large sizes completely covers vertically grown nanorods. After the secondary synthesis, the sizes of nanostructures and their density increased. XRD pattern and SEM images show that the synthesized ZnO microrods have high crystallinity.

PL spectrum of the first synthesis ZnO NRs of sample No.1 consists of two peaks: narrow and weak at 390 nm with strong and broad emission band at 570 nm. After secondary synthesis of nanorods, the ratio of the intensity of the ultraviolet emission to the intensity of the broadband (visible) emission Iuv/Iv decreased 2 times (Fig. 3a). In addition, the position of the peak’s maxima remained approximately unchanged. PL spectrum of the first synthesis sample No2 also consists of two bands: strong and narrow at 386 nm with slight deviations and wide with a maximum at around 570 nm (Fig. 2). Unlike the sample No1, after secondary synthesis sample No2, the position of the peak’s maxima was red-shift to almost 5 nm (insert Fig.3 b) and the ratio of the intensity of the UV to the intensity of the broadband (visible) emission Iuv/Iv decreased 3 times (Fig. 2a).

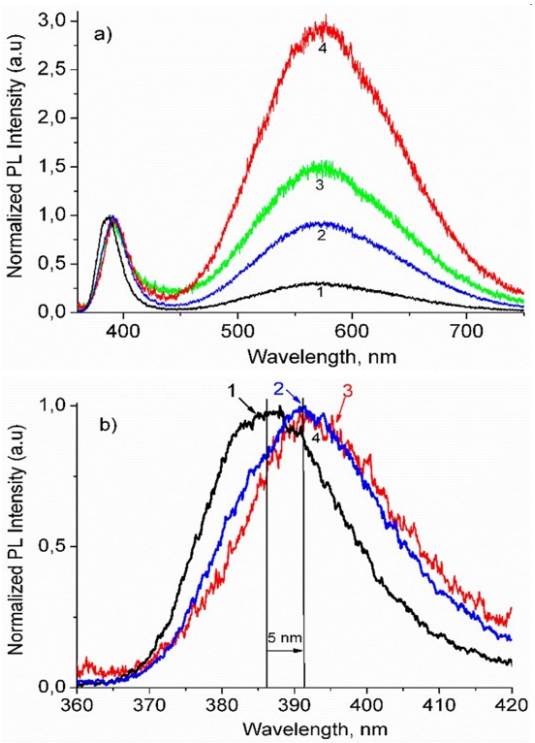

Figure 3. a) Photoluminescence spectra of ZnO nanorods obtained after the first and secondary synthesis of Samples: curves 1, 2 - sample No.2 and curves 3, 4 belong to sample No.1, respectively. b) The UV peak position of samples after secondary synthesis.

Discussion:

UV peak is attributed to the near band edge (NBE) luminescence of zinc oxide, namely, the emission of a free exciton [14,16]. Considering that ZnO nanorods were synthesized without extraneous additions, the yellow-orange luminescence bands in the region of 570 nm can be attributed to intrinsic defects and their complexes. Since ZnO microrods are synthesized by hydrothermal method, we can consider the synthesis process as an environment rich in oxygen atoms. Theoretical calculations show that the formation energy of zinc vacancies (2,1-2,3 eV) and interstitial oxygen atoms (1,3-1,6 eV) in the crystal structures of nanomaterials synthesized in such environments is smaller than other defects, and they dominate among native defects [17]. The yellow-orange band is often observed in zinc oxide nanomaterials grown from aqueous solutions at relatively low temperatures and is usually attributed to interstitial oxygen or complexes formed with the participation of oxygen [15,16]. We assume that the difference in UV peak positions in the samples may be due to differences in the sizes of vertically grown and horizontally deposited nanorods on the surface of the substrates. Therefore, in sample No.1, the proportion of the upper layer plays a major role in the emission distribution because of upper layer is covered the surface of the substrate at any time and the maximum of the UV band is located on the large wavelength side. However, in sample No.2, due to the vertical placement of the substrate admit to synthesis of nanostructures over the entire volume of the solution simultaneously with the growth of nanorods on the seed layer. Therefore, the UV peak position of the first-time synthesis sample No.2 is located at 386 nm. After secondary synthesis sample No.2, nanorods the nanorods continue to grow from the continuation of the nanorods formed in the first synthesis, as a result their size increases and the position of the UV peak maxima was red-shift to the peak maximum of sample No.1. If the nanorods were synthesized in the autoclave for a second time to synthesize ZnO nanorods, their size increased. At the same time, the photoluminescence spectra of the samples showed an increase in the emission band associated with defects. Considering that the defect observed in the PL spectrum is interstitial oxygen, the increase in the emission band corresponding to this defect in the doubly synthesized samples indicates that they are a bulk defect.

Conclusions

ZnO nanostructures were synthesized on a stainless-steel mesh using a low-temperature hydrothermal method. The nanostructures completely cover the wire surface and form a structure consisting of two layers: vertically grown nanorods are located below, and horizontally located nanorods are "piled" on top. The nanorods exhibit strong exciton luminescence, indicating their good quality. If the nanorods were synthesized in the autoclave for a second time to synthesize ZnO nanorods, their size increased. At the same time, the photoluminescence spectra of the samples showed an increase in the emission band associated with defects. Considering that the defect observed in the PL spectrum is interstitial oxygen, the increase in the emission band corresponding to this defect in the doubly synthesized samples indicates that they are a bulk defect.

Authors' contribution.

Conceptualization, J.R.; methodology, R.B.; formal analysis, R.B.; investigation, J.R.; data curation, B.R.; writing—original draft preparation, J.R.; writing—review and editing, J.R.; ll authors have read and agreed to the published version of the manuscript.

Funding source.

There is no funding source.

Ethics approval.

Not applicable. This study did not involve humans or animals.

Consent for publication.

Not applicable. This study did not involve human participants, and therefore, informed consent was not required.

Data Availability Statement

The data supporting the reported results are available upon reasonable request from the corresponding author.

Acknowledgments

The Foundation for Basic Research of the Academy of Sciences of Uzbekistan: "Research of crystallographic, spectral-absorption, spectral-luminescence, photocatalytic and electronic properties of nanomaterials containing atoms of noble metals and the factors affecting them".

Conflict of interest

The authors declare no conflicts of interest. The funders had no role in the design of the study; in the collection, analyses, or interpretation of data; in the writing of the manuscript; or in the decision to publish the results.

Abbreviations

ZnO	Zinc oxide
PL	Photoluminescenced
SEM	Scanning electron microscope
NBE	near band edge
UV	ultraviolet

References

[1] Abdelkarem K., Saad R., El Sayed A.M., Design of high-sensitivity La-doped ZnO sensors for CO2 gas detection at room temperature. Sci Rep 13, 18398 (2023). https://doi.org/10.1038/s41598-023-45196-y

[2] Rabisankar Dash, C. Mahender, Prasanta Kumar Sahoo, Ankur Soam, Preparation of ZnO layer for solar cell application, Materials Today: Proceedings, Volume 41, Part 2, 2021, Pages 161-164, https://doi.org/10.1016/j.matpr.2020.08.448.

[3] A. Esbergenova, Interlinking the Fe doping concentration, optoelectronic properties, and photocatalytic performance of ZnO nanostructures, Curr. Appl. Phys. 2024, 67 18–29. https://doi.org/10.1016/j.cap.2024.07.009.

[4] Zhuxin Li, Wei Liu, Ru Wang, Feng Chen, Jinping Chen, Yizhi Zhu, Zengliang Shi, Chunxiang Xu, Interface design for electrically pumped ultraviolet nanolaser from single ZnO-nanorod, Nano Energy, Volume 93, 2022, 106832, https://doi.org/10.1016/j.nanoen.2021.106832.

[5] Rodrigues J., Pereira S.O., Zanoni J., Rodrigues C., Brás M., Costa F.M., Monteiro T., ZnO Transducers for Photoluminescence-Based Biosensors: A Review. Chemosensors 2022, 10, 39. https://doi.org/10.3390/chemosensors10020039.

[6] Sagnik D., Uttam K.G., Rajib D., Chandan K.G., Mrinal P. White light phosphorescence from ZnO nanoparticles for white LED applications, New J. Chem., 2022,46, 17585-17595, https://doi.org/10.1039/D2NJ02684H.

[7] Dhirendra Kumar Sharma, Sweta Shukla, Kapil Kumar Sharma, Vipin Kumar, A review on ZnO: Fundamental properties and applications, Materials Today: Proceedings, Volume 49, Part 8, 2022, Pages 3028-3035, https://doi.org/10.1016/j.matpr.2020.10.238.

[8] Xie J, Li H, Zhang T, Song B, Wang X, Gu Z. Recent Advances in ZnO Nanomaterial-Mediated Biological Applications and Action Mechanisms. Nanomaterials (Basel). 2023 Apr 27;13(9):1500. https://doi.org/10.3390/nano13091500.

[9] Eric Navarrete, Frank Güell, Paulina R. Martínez-Alanis, Eduard Llobet, Chemical vapour deposited ZnO nanowires for detecting ethanol and NO2, Journal of Alloys and Compounds, Volume 890, 2022, 161923, https://doi.org/10.1016/j.jallcom.2021.161923.

[10] R.R. Jalolov, B.N. Rustamova, Sh.Z. Urolov, Z.Sh. Shaymardanov, High-temperature photoluminescence properties of various defects in hydrothermally grown ZnO microrods. Physica B 675 (2024) 415613. https://doi.org/10.1016/j.physb.2023.415613.

[11] José Luis Clabel Huamán and Victor Anthony Garcia Rivera. Perovskite Ceramics Recent Advances and Emerging Applications (Elsevier, 2023). https://doi.org/10.1016/C2020-0-03937-X.

[12] R.R. Jalolov, Sh.Z. Urolov, Z.Sh. Shaymardanov, S.S. Kurbanov, B.N. Rustamova, Complex features of the photoluminescence from ZnO nanorods grown by vapor-phase transport method, Materials Science in Semiconductor Processing 128 (2021) 105783. https://doi.org/10.1016/j.mssp.2021.105783.

[13] K. Punia G., Lal S.Dalela, A comprehensive study on the impact of Gd substitution on structural, optical and magnetic properties of ZnO nanocrystals, Journal of Alloys and Compounds 868 (2021) 159142. https://doi.org/10.1016/j.jallcom.2021.159142.

[14] Tokimori S., Funato K., Wada K., Matsuyama T., Okamoto K., Emission Enhancement of ZnO Thin Films in Ultraviolet Wavelength Region Using Au Nano-Hemisphere on Al Mirror Structures. Nanomaterials 2025, 15, 400. https://doi.org/10.3390/nano15050400.

[15] A.C. García-Velasco, A. Báez-Rodríguez, M. Bizarro, R.M. Calderón-Olvera, J. Hernández-Torres, L. García-González, L. Zamora-Peredo, Surface defect-rich ZnO nanostructures with high yellow-orange luminescence, Journal of Luminescence, Volume 251,2022, 119187, https://doi.org/10.1016/j.jlumin.2022.119187.

[16] Kumar N., Poulose V., Laz Y.T., Chandra F., Abubakar S., Abdelhamid A.S., Alzamly A., Saleh N., Temperature Control of Yellow Photoluminescence from SiO2-Coated ZnO Nanocrystals. Nanomaterials 2022, 12, 3368. https://doi.org/10.3390/nano12193368.

[17] Cai-Qin L., Si-Cong Z., Chi-Hang L., Francis Chi-Chung L., Ferromagnetic behavior of native point defects and vacancy-clusters in ZnO studied by first principle calculation, Mater. Res. Express. 2020. Vol. 7. 076103. https://doi.org/10.1088/2053-1591/aba14a.